Valence Band Photoemission Studies of Corrosion Inhibitor Action on Iron Surfaces: Effect of Etidronate

Ian D. Welsh and Peter M. A. Sherwood*

Department of Chemistry, Willard Hall, Kansas State University, Manhattan, Kansas 66506

Received July 22, 1991. Revised Manuscript Received October 3, 1991

Valence band X-ray photoelectron spectroscopy is used to examine the interaction between the corrosion inhibitor calcium etidronate (etidronic acid is hydroxyethylidene diphosphonic acid, HEDP) and iron and mild steel surfaces. It is found that the inhibitor is probably oxidized on interaction with the native oxide film on the metal surface to give ferrous phosphate under an outer layer of iron etidronate. The outer iron etidronate layer probably contains iron in a tetrahedral environment. The surface film is amorphous and increases in thickness with exposure time. The valence band spectra of calcium etidronate, iron etidronate, and ferrous and ferric phosphate are interpreted by spectra calculated using Xα calculations. The changes caused by the examination of these samples by X-ray photoelectron spectroscopy is monitored by X-ray diffraction, which indicates that samples are dehydrated and sometimes converted from crystalline to amorphous forms by spectroscopic examination. The principal changes resulting from spectroscopic examination appears to be caused by the ultrahigh vacuum conditions and the heat from the X-ray gun, since the effect can be reproduced by heating the samples in a vacuum oven.

Introduction

There has been considerable interest in the nature of the surface films of corrodible metals and the effect that corrosion inhibitors have on these films. Corrosion inhibitors may form a specific film on a metal surface, and may cause changes in the surface oxide film. Ideally, a corrosion inhibitor would remove any unwanted and unprotective oxide layer and form an impervious and stable protective film on the metal surface. To understand the action of the inhibitor, it is essential to be able to identify the chemical composition of the film formed.

Surface analytical techniques have been widely used to investigate such films (see ref 1 and the references therein), and X-ray photoelectron spectroscopy (XPS or ESCA) has been one of the most widely used methods. Many of the previous XPS studies have concentrated on the use of core chemical shift information to provide chemical information about inhibitor films. In an earlier paper[1] we reviewed many of these studies. In this work we concentrate on the role of the organophosphorus compound, etidronic acid. This substance has found widespread use as a corrosion inhibitor in paints, for use in boiler water treatments[2-4] coatings, as a complexing agent, as a water softener, and as an electropolishing sequestering agent for copper and an electroplating complexing agent for various metals.[5] Its role as a corrosion inhibitor for iron and steel has been widely investigated.[6-8] In particular it has been found that etidronic acid derivatives can chemically interact at low concentrations with steel.[5] The combination of etidronates with other inhibitors has also found to be valuable.[6,7] In our earlier work[1] we reported a valence band study of etidronic acid ($C_2P_2O_7H_8$) and its salts, with the valence band data interpreted by Xα calculations.

Our earlier work focused on the changes that occur when iron and mild steel are exposed to calcium etidronate solution. The main conclusion was that there was an etidronate-rich surface film, which could be removed by argon ion etching to give increasing amounts of iron oxide (FeOOH and Fe_2O_3). In this paper we report an extension of this earlier work and discuss how subtle changes in the nature of the surface films formed can be observed, which aid us in understanding the role of the inhibitor in this situation. In particular we report an interaction between the inhibitor film and the normal oxidized iron surface, and we examine the effect of placing various samples into the UHV of the XPS chamber.

Experimental Section

The X-ray photoelectron (XPS or ESCA) spectra were collected on an AEI (Kratos) ES200B X-ray photoelectron spectrometer with a base pressure of about 10^{-9} Torr. The spectrometer was operated in the fixed retardation ratio (FRR) mode (ratio 1:23) using Mg or Al $K\alpha_{1,2}$ X-ray radiation (240 W). Analyzer resolution was of the same order as the X-ray line width (0.7 eV). Typical data collection times were 10-20 h for the valence band and 1-3 h for the core regions. The spectrometer energy scale was calibrated using copper[9] and the separation (233 eV) between photoelectron peaks generated by Mg and Al $K\alpha_{1,2}$ X-rays.

Etidronic acid (1-hydroxyethylidene diphosphonic acid (HEDP)) was obtained from Monsanto and was purified by passing through activated charcoal. Calcium etidronate was obtained from International Paint, and iron(III) etidronate was obtained as a precipitate formed after reacting mild steel with dilute etidronic acid for 5 days. Calcium phosphate ($Ca_{10}(OH)_2(PO_4)_6$) as obtained from Baker, iron(II) ($Fe_3(PO_4)_2 \cdot 8H_2O$) and iron(III) phosphate ($FePO_4 \cdot 2H_2O$) from Pfaltz and Bauer, and lithium phosphate from AESAR. Pure iron (99.99% purity) was obtained from Goodfellows Metals. The mild steel sample was a commercial sample. The samples were polished with emery paper and alumina. No trace of aluminum was found on the plished metal on XPS examination. The metals thus had only an air-formed film on them. Films formed by exposure to calcium etidronate solution on the iron or mild steel surfaces were depth profiled by argon ion etching using an Ion Tech B22 saddle-field ion gun at 5 kV and 1 mA. Saturated calcium etidronate solution (about 1 mM) using quadruply distilled water was used for the exposure experiments.

(1) Welsh, I. D.; Sherwood, P. M. A. *Proc. Electrochem. Soc.* **1989**, *89-13* (Advances in Corrosion Protection by Organic Coatings; Scantelbury, D., Kendig, M., Eds.), 417.
(2) Good, R. D.; Arots, J. B. *Proc. Int. Water Conf. Eng. Soc. West. Pa.* **1981**, *42*, 65.
(3) Pallos, G.; Wallwork, G. *Corros. Rev.* **1985**, *6*, 237.
(4) Bohnsack, G.; Lee, K. H.; Johnson, D. A.; Buss, E. *Mater. Perform.* **1986**, *5*, 32.
(5) Fang, J. L.; Wu, N. J. *J. Electrochem. Soc.* **1989**, *136*, 3800.
(6) Sekine, I.; Hirakawa, Y. *Corrosion* **1986**, *42*, 272.
(7) Airey, K.; Armstrong, R. D.; Handyside, T. *Corros. Sci.* **1988**, 449.
(8) Armstrong, R. D.; Airey, K.; Su, F. *Electrochim. Acta* **1989**, *34*, 707.
(9) Annual Book of ASTM Standards, Vol. 03.06, Published in *Surf. Interface Anal.* **1988**, *11*, 112.

0897-4756/92/2804-0133$03.00/0

Table I. Parameters Used and Features of the Xα Calculations

α Values: phosphorus 0.72620, oxygen 0.74447, iron 0.71150
outer = intersphere 0.74082 (PO_4^{3-}), 0.73806 (FeO_4^{5-}), 0.73700 (FeO_6^{9-})

maximum l value[a]	phosphorus 3	iron 2	oxygen 1
cluster	PO_4^{3-}	FeO_4^{5-}	FeO_6^{9-}
sym	T_d	T_d	O_h
P–O bond length, Å	1.560		
Fe–O bond length, Å		1.853	2.030
phosphorus sphere radius, Å	0.991		
iron sphere radius, Å		1.204	1.300
oxygen sphere radius, Å	0.959	1.112	1.237
Watson sphere radius, Å	1.560	1.853	2.030
outer-sphere radius, Å	2.519	2.965	3.267
virial ratio ($-2T/V$)	1.001398	1.000943	1.002105

convergence: when the difference in potentials at the beginning and end of the iteration were less than 10^{-5} of the potential at the start of the iteration; this gives energy levels that differed by less than 10^{-6} Rydberg between the last two iterations.

core electrons: "thawed" so that they retained atomic character while being fully included in the iterative process; phosphorus 1s, 2s, and 2p electrons and oxygen 1s electrons were treated as core electrons.

[a] Outer 3.

Valence band XPS data are shown after removal of a nonlinear background (using our previously described method[10,11]), so that the spectra can be conveniently compared with the calculations. While any background subtraction method requires caution, the removal of this background had no substantial effect on the features of the reported spectra.

The spectra of phosphate and etidronate compounds were calibrated against residual hydrocarbon with a C(1s) binding energy of 284.6 eV. The Ca(3p) binding energy was found to be at 26.3 eV in both the phosphate and etidronate spectra, and this was used as an internal calibrant for the valence band spectra of metal exposed to calcium etidronate solution. Since such calibration involved an internal calibrant and thus the measure of the separation of the appropriate peak from the Ca(3p) peak (the most intense feature in the valence band region), binding energy values are considered to be consistent to ±0.05 eV.

Multiple-scattered wave Xα calculations were used to calculate the XPS valence band spectra. For each energy level a percentage of the occupancy of the level corresponding to each atom in the molecule is obtained from the calculation. Calculated spectra can be generated by adding together a number of component peaks corresponding to the calculated energy levels (or some combination of closely spaced energy levels). Each peak has a position corresponding to the calculated energy level and an intensity (area) corresponding to the number of electrons in the energy level multiplied by the atomic population for the level, adjusted by the appropriate atomic photoelectric cross section (using the values calculated by Scofield[12]). Each component in the calculated spectrum corresponds to a 50% Gaussian–Lorentzian product function,[10,1] with each peak having the same full width at half-maximum (fwhm) and an area generated as described above including X-ray satellite features for the X-radiation used. Table I shows the input parameters and calculation features for the calculations, details for the etidronate ion being reported previously.[1] The PO_4^{3-} cluster in Table I was calculated using the transition-state method, which means that half an electron is removed from each energy level to account for ionization in a series of different calculations, one for each energy level.

X-ray diffraction (XRD) studies were carried out with a Scintag XDS 2000 instrument. The X-ray radiation wavelength used was Cu $K\alpha_1$ (0.154059 nm) with an X-ray energy of 1800 W. The data were collected using the step-scanning mode with a step size of 0.03–0.005°. Samples were normally mounted in a Mylar tray. The angle of the X-rays with respect to the sample surface was fixed (fixed-ω scan) and was set to 2° in Figure 1 and 5° in the other figures.

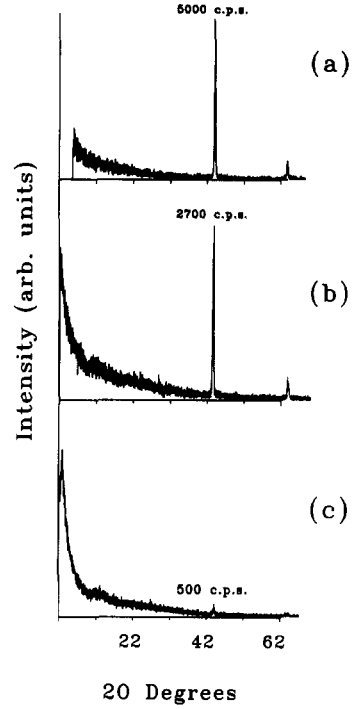

Figure 1. X-ray diffraction patterns of the calcium etidronate treated plate: (a) steel plate with no exposure; (b) steel plate after 2 weeks of exposure; (c) polished iron plate after 124 days of exposure. The spectra were collected for similar time periods, and the counts corresponding to the 44° peak due to α-iron are indicated on the spectrum. Note how the background increases from a to c relative to the iron peaks.

Results and Discussion

In this paper we will discuss only the valence band XPS data. A full set of core XPS data were recorded, but these data added nothing significant that was not reported in our previous work.[1]

Let us start by examining the effect of exposing iron or mild steel to calcium etidronate solution. In our earlier work[1] we found that the film formed was much thinner when the metal sample was polished before use, and in this work all samples exposed for 2 h and 124 days were polished before exposure. In all cases the films formed after exposure (including all the argon ion etched films discussed here) showed the presence of phosphorus and calcium as indicated by the P(2p) and Ca(2p) core regions (and the Ca(3p) region of the valence band). Our previous studies[1,13] indicated that the Fe(2p) core region shows little difference between oxidized iron and an iron etidronate complex.

Film Thickness. Visible opalescent film formation could be seen on the samples exposed for 2 weeks and 124 days, and the film was visibly thick on the samples exposed to calcium etidronate for 124 days. While this indicates considerable activity, we still describe calcium etidronate as an inhibitor in the sense that an identical metal sample exposed to quadruply distilled water for the same period always showed considerably more corrosion with flakes of brown gelatinous rust. The film appeared visibly regular. No differences were seen between the pure iron plate and the mild steel plates, but this study focuses on the chemistry of the films seen and not differences between iron and

(10) Sherwood, P. M. A. *Practical Surface Analysis by Auger and Photoelectron Spectroscopy*; Briggs, D., Seah, M. P., Eds.; Wiley: London, 1983; Appendix 3.

(11) Sherwood, P. M. A. *Practical Surface Analysis, Vol 1: Auger and X-ray Photoelectron Spectroscopy*, 2nd ed.; Briggs, D., Seah, M. P., Eds.; Wiley, London, 1990; Appendix 3.

(12) Scofield, J. H. *J. Electron Spectrosc.* **1976**, *8*, 129.

(13) Welsh, I. D.; Sherwood, P. M. A. *Phys. Rev. B* **1989**, *40*, 6386.

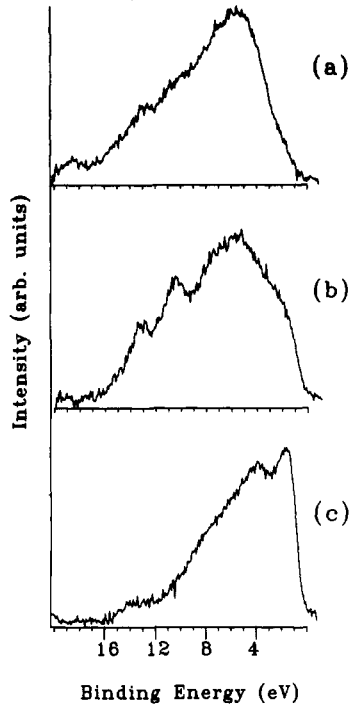

Figure 2. Valence band XPS spectra for the calcium etidronate treated polished mild steel plate: (a) after 2 h of exposure; (b) as (a) after a 2-min argon ion etch; (c) as (b) after a further 4-min argon ion etch (total etch time 6 min).

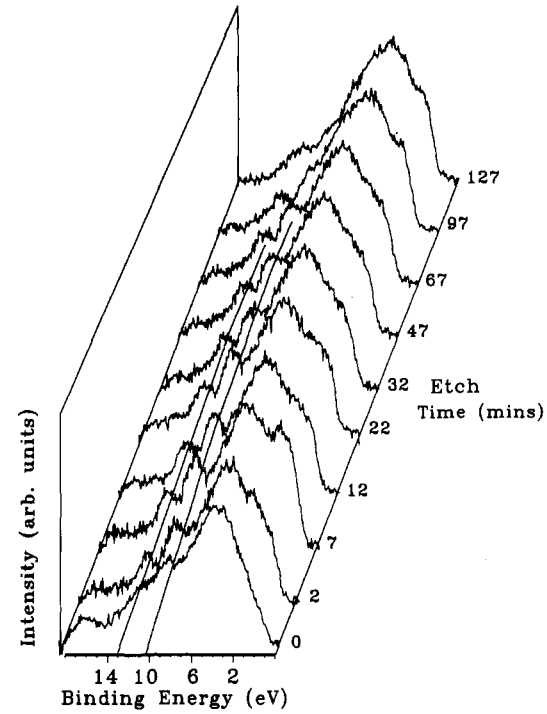

Figure 3. Valence band XPS spectra for the 2-week exposed calcium etidronate treated mild steel plate after different total argon ion etch times. Phosphate features at 10.3 and 13.0 eV are shown as connecting lines.

steel which would require a study of iron and steel samples under identical conditions. The mild steel sample showed an XPS spectrum identical to that of metallic iron.

Figure 1 shows the X-ray diffraction patterns of the mild steel and films formed after 2 weeks and 124 days. The two sharp features at 2θ of 44 and 64 correspond to that of metallic iron (α-iron). The reduction in intensity of these features indicates the increasing film thickness with exposure time. Thus a crude measure of this increasing thickness can be seen by comparing the intensity of the peak at 44°, 5000, 2700, and 500 counts in Figure 1a–c, respectively. If one assumes an air-formed film thickness on mild steel of about 50 Å, then the film formed after two weeks exposure is at least 100 Å, and after 124 days exposure at least 500 Å. The etching experiments on the 2-week exposure film suggest a thickness greater than 100 Å (at least 250 Å on the basis of reasonable etch rates), but the estimates above are very crude since the attenuation of the signal by the overlayer will depend upon the composition of the overlayer. It can also be seen that the film formed is amorphous, there being no other sharp features in the diffractogram, and some broad humps characteristic of an amorphous film.

Phosphate Formation. Examination of the valence band XPS data for these three exposure times (Figures 2–4) provides more information. In the case of short (2 h) and medium (2 week) exposure times the spectrum changes significantly after 2 min of argon ion etching (Figure 2b and Figure 3). The most noticeable feature is the appearance of two sharp peaks at 10.3 and 13 eV binding energy in many of the spectra. In the long (124 day) exposure time experiment no marked change is seen with etch time. The features at 10.3 and 13 eV were internally calibrated and were found to be present in nearly all the spectra shown in Figure 3 (and thus can be used as a scale indicator).

Let us first examine the origin of the two sharp peaks at 10.3 and 13 eV binding energy. These features are strongly indicative of phosphate. While phosphate and

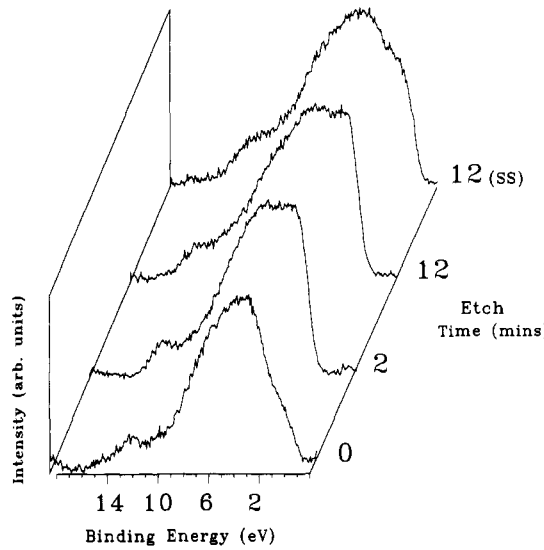

Figure 4. Valence band XPS spectra for the 124 day exposed calcium etidronate treated polished iron plate after different total argon ion etch times.

etidronate cannot be distinguished in the core region (P(2p), O(1s)), they are very different in the valence band region, as Figures 5 and 6 indicate for calcium etidronate and calcium phosphate. Figure 5 includes the intense Ca(3p) feature at 26.3 eV binding energy which has been used as an internal standard for all the spectra. This feature was found in all the valence band spectra of the etched exposed metal samples, with the Ca(3p) intensity falling with etch time. The calculated spectra for the etidronate and phosphate (Figure 5b,d) and (d)) show the Ca(3p) feature as the intense peak at highest binding energy. It will be seen that there are features due to the etidronate (C(2s) and O(2s) character) and phosphate (O(2s) character) groups that overlap the Ca(3p) region, and the Ca(3p) and core Ca(2p) regions showed a substantial

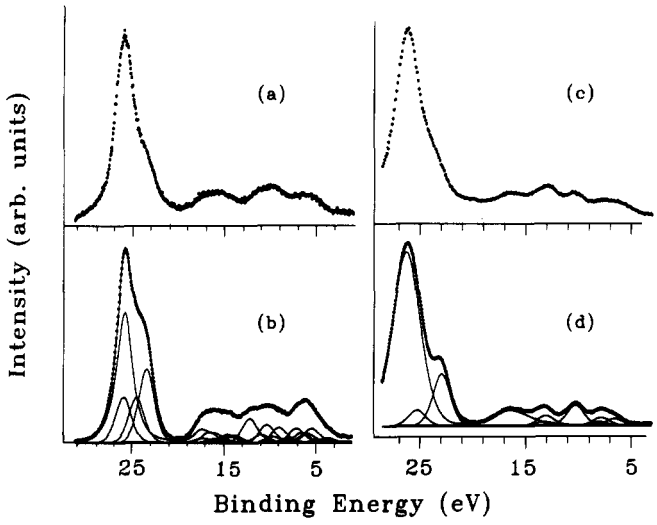

Figure 5. Wide range valence band XPS spectra for (a) calcium etidronate, and (c) calcium phosphate. The corresponding spectra calculated from Xα calculations are shown in (b) for calcium etidronate and in (c) for calcium phosphate.

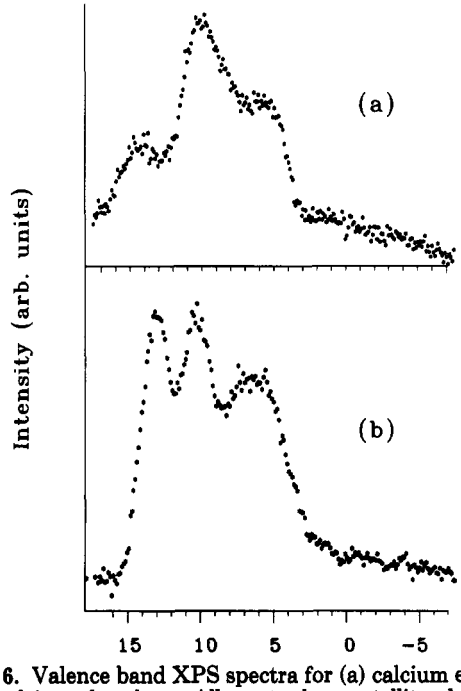

Figure 6. Valence band XPS spectra for (a) calcium etidronate and (b) calcium phosphate. All spectra have satellites due to $K\alpha_{3,4}$ components removed.

reduction in the amount of calcium in the film after long etch times. Figure 5, which includes features from $K\alpha_{3,4}$ X-ray satellite radiation photoemission from the intense Ca(3p)/O(2s) region, shows a clear difference in the spectrum of phosphate and etidronate. The figure shows a spectrum with three broad peaks for the calcium etidronate and four significantly narrower peaks for calcium phosphate in the low binding energy (<19 eV) valence band region. The peak in both spectra at a binding energy of about 16 eV contains a substantial (in the case of phosphate entire) contribution from $K\alpha_{3,4}$ X-ray satellite radiation photoemission from the intense Ca(3p)/O(2s) region. The position of this contribution shifts slightly on changing the X-radiation from magnesium to aluminum, but in both cases the overall spectral appearance is similar. Figure 6 shows the low binding energy valence band region for calcium etidronate and calcium phosphate with the X-ray satellite features removed. The valence band region

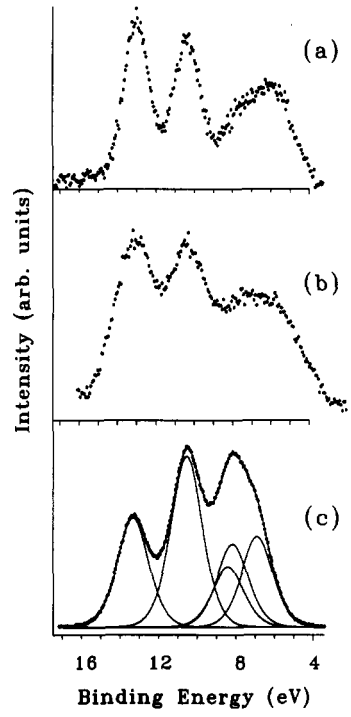

Figure 7. Valence band XPS spectra for (a) lithium phosphate (Li_3PO_4) and (b) calcium phosphate ($Ca_{10}(OH)_2(PO_4)_6$), compared to the spectra (c) generated from an Xα calculation on the PO_4^{3-} ion. The component energy levels are shown in (c). All spectra have satellites due to $K\alpha_{3,4}$ components removed.

for phosphate can be understood by comparing the spectrum of phosphates with the calculated spectrum for an Xα calculation as shown in Figure 7. The spectra of phosphates has been extensively investigated experimentally and theoretically (refs 14–26 provide representative examples of earlier work), and our data are in good agreement with previously reported phosphate spectra.

In the phosphate spectra in Figure 7 the two features at 10.3 and 13 eV can clearly be seen (the calculation shows these features separated by a slightly larger (by 0.12 eV) binding energy with an intensity that is too low for the high binding energy peak—as with any calculation extract agreement can rarely be expected). Figure 8 compares the spectrum of the calcium etidronate treated polished mild steel plate after a 2-h exposure and 2 min of argon ion etching with that of ferrous phosphate and calcium etidronate. The two features at 10.3 and 13.0 eV due to phosphate are clearly present in Figure 8a,b, but *no feature at 13.0 eV is seen in Figure 8c, and indeed a valley is seen in the spectrum at this binding energy.* The difference

(14) McAloon, B. J.; Perkins, P. G. *Theor. Chim. Acta* **1971**, *22*, 304.
(15) Connor, J. A.; Hillier, I. H.; Wood, M. H.; Barber, M. *J. Chem. Soc., Faraday Trans. 2* **1974**, *70*, 1040.
(16) Hollinger, G.; Bergignat, E.; Joseph, J.; Robach, Y. *J. Vac. Sci. Technol. A* **1985**, *3*, 2082.
(17) Connor, J. A.; Hillier, I. H.; Saunders, V. R.; Barber, M. *Mol. Phys.* **1972**, *23*, 81.
(18) Uchtman, V. A.; Gloss, R. A. *J. Phys. Chem.* **1972**, *76*, 1298.
(19) Johansen, H. *Theor. Chim. Acta* **1974**, *32*, 273.
(20) Prins, R. *J. Chem. Phys.* **1974**, *61*, 2580.
(21) Weber, J. *Chem. Phys. Lett.* **1976**, *40*, 275.
(22) Kosuch, N.; Tegeler, E.; Wiech, G.; Faessler, A. *Chem. Phys. Lett.* **1977**, *47*, 96.
(23) Rizkalla, E. N. *Inorg. Chim. Acta* **1982**, *60*, 53.
(24) Sayarh, A.; Lhamyani-Chraibi, M.; Arriau, J.; Weber, J. *J. Mol. Struct.* **1986**, *139*, 25.
(25) Le Beuze, A.; Lissillour, R.; Quemerais, A.; Agliz, D.; Marchand, R.; Chermette, H. *Phys. Rev. B* **1989**, *39*, 11055.
(26) Sferco, S. J.; Allan, G.; Lefebvre, I.; Lannoo, M.; Bergignat, E.; Hollinger, G. *Phys. Rev. B* **1990**, *42*, 11232.

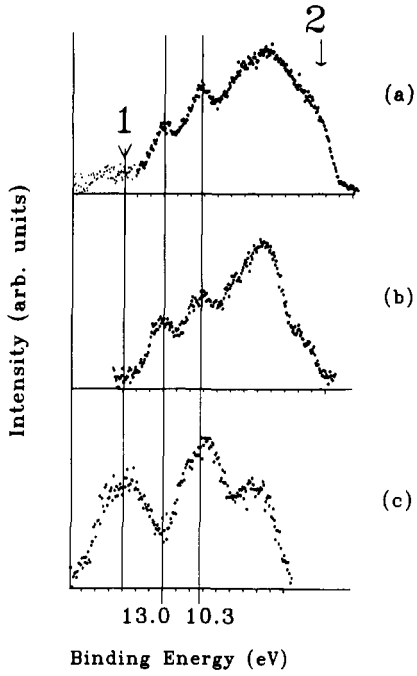

Figure 8. Valence band XPS spectra for (a) the calcium etidronate treated (2 h) polished mild steel plate after a 2-min etch, (b) ferrous phosphate ($Fe_3(PO_4)_2 \cdot 8H_2O$), and (c) calcium etidronate. The two phosphate features at 13 and 10.3 eV are seen in a and b. Feature 1 is mainly due to $K\alpha_{3,4}$ intensity from the Ca(3p) region. Feature 2 is probably an excess of Fe(II).

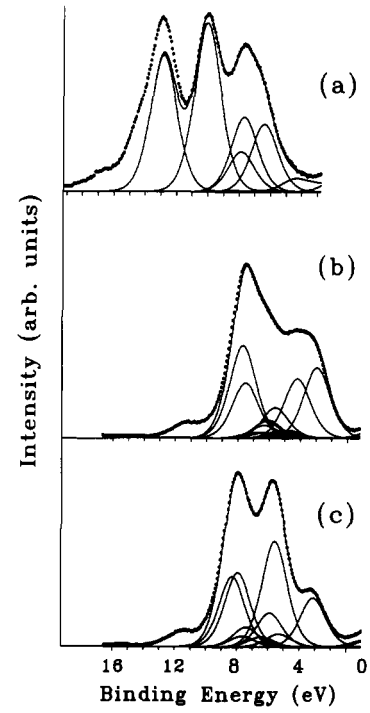

Figure 9. Valence band XPS spectra calculated from Xα calculations: (a) PO_2 unit in the phosphates; (b) FeO_2 tetrahedral unit; (c) FeO_2 octahedral unit. All spectra have satellites due to $K\alpha_{3,4}$ components (from the O(2s) region) included.

between the etidronate spectrum is clearly seen, in both the separation of the two peaks at highest binding energy (16 and 10 eV in the case of etidronate) and the difference in width of the peaks. The difference in width of the peaks is expected, since the calculation of the etidronate spectrum (Figure 11) clearly shows that the peaks are made up of a number of overlapping features due to different energy levels, rather than the single energy levels that give rise to the peaks in phosphate. Features excited by X-ray satellite radiation are not removed in Figure 8, and this gives rise to the features at position 1. All spectra in Figure 8 were obtained using Mg X-radiation. In Figure 8a the lightly dotted region of the spectrum comes entirely from the Ca(3p)/O(2s) region satellites and in Figure 8c substantial intensity comes from this source. This explains the difference between Figures 8c and 11a where features due to satellites were removed. We thus conclude that the features at 10.3 and 13.0 eV are conclusive evidence for the presence of phosphate.

We were careful to check that the observation of phosphate was not simply a result of decomposition by argon ion etching of an outer etidronate layer. We argon ion etched calcium etidronate and iron etidronate for 2–3 min and could find no significant difference in the spectra. Thus we conclude that the observation of phosphate can reasonably be attributed to a chemical interaction between the etidronate and the native oxide layer on the metal.

Iron Phosphate Spectra. It is interesting to investigate the type of phosphate found in many of the spectra (Figure 2b and many spectra in Figure 3) resulting from argon ion etching of metal treated by calcium etidronate. Both iron(II) and iron(III) phosphate are well-known. Both phosphates are hydrated, and have a range of possible structures.[27] Iron(II) phosphate is known as the monoclinic form *vivianite*, $Fe_3(PO_4)_2 \cdot 8H_2O$ where iron is surrounded octahedrally by oxygens. In *ludlamite*, $Fe_3(PO_4)_2 \cdot 4H_2O$ iron is also octahedrally surrounded by oxygens. Iron(III) phosphate is best known as *metastrengite*, $FePO_4 \cdot 2H_2O$ where the iron is again surrounded by an octahedral arrangement of oxygens with an average Fe–O distance[28] of 2.03 Å (the same as in Fe_2O_3). The related compound *strengite* is also known which is orthorhombic rather than monoclinic with the same octahedral geometry around iron. The anhydrous material $FePO_4$ has a tetrahedral arrangement of oxygen atoms around the iron. To understand the spectra obtained we have generated an iron(III) phosphate spectrum by combining the calculated spectrum for a PO_2 unit with that of either an octahedral FeO_2 unit or a tetrahedral FeO_2 unit (Figure 9). The spectra obtained (Figure 10) can be compared with the observed spectra for vivianite and metastrengite. In comparing iron(III) and iron(II) phosphates, the main difference is the relative increase in the intensity of the Fe(3d) features due to the stoichiometric increase in the amount of iron, together with an increase in the intensity of low binding energy features (since iron(II) has one more Fe(3d) electron in the highest occupied orbital in the outer valence band region). Otherwise the spectrum appears much the same. The generated spectrum for octahedral iron shows two prominent features around 5–7 eV binding energy, whereas the spectrum for tetrahedron iron has only one feature. The experimental data (Figure 2b and many spectra in Figure 3) certainly correspond to multiple features in this region, and we thus feel that they are more likely to correspond to iron in its octahedral form. Of course this would be expected from the discussion above, but one needs to consider possible alteration of the compounds during examination in the spectrometer. This consideration will be discussed in more detail below.

Etidronate Spectra. The spectrum obtained of the treated metal before etching corresponds to etidronate, a

(27) Wycoff, R. W. G. *Crystal Structures*, 2nd ed.; Interscience: New York, 1963; Vol. 4.

(28) Moore, P. B. *Am. Mineral.* **1966**, *51*, 168.

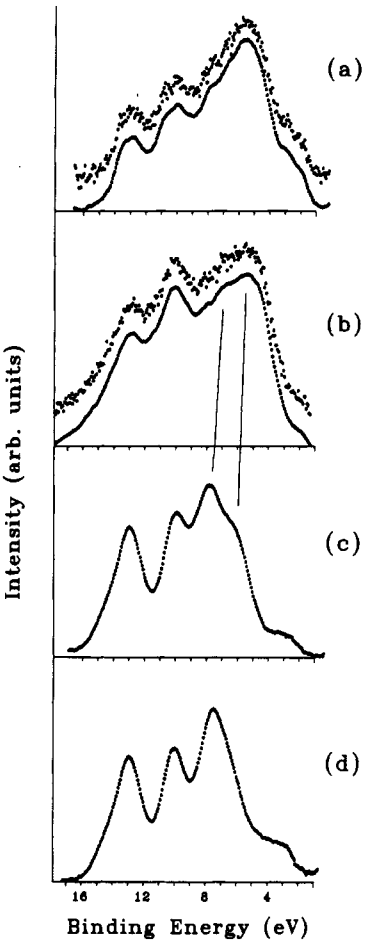

Figure 10. Valence band XPS spectra for (a) ferrous phosphate ($Fe_3(PO_4)_2 \cdot 8H_2O$), and (b) ferric phosphate ($FePO_4 \cdot 2H_2O$), compared to the spectra generated from the Xα calculations by (c) combining the PO_2 unit with the octahedral FeO_2 unit, and by (d) combining the PO_2 unit with the tetrahedral FeO_2 unit. (a) and (b) both have smoothed spectra shown under the original experimental data.

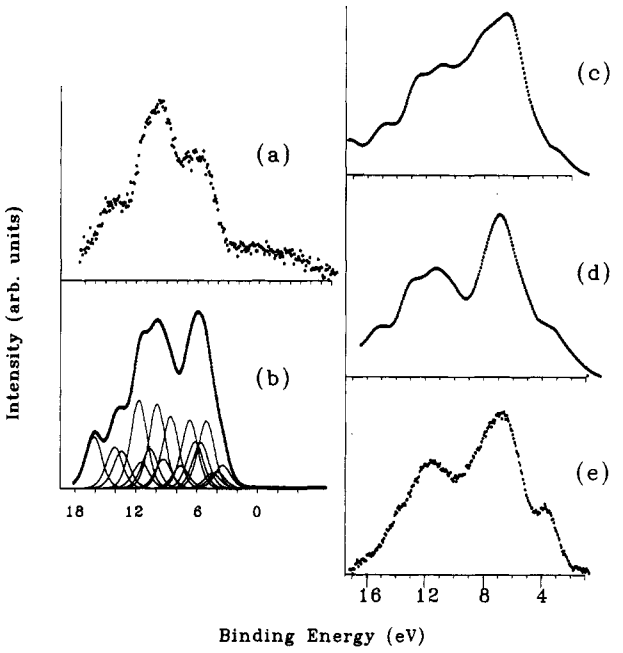

Figure 11. Valence band XPS spectrum for (a) calcium etidronate compared to the spectrum (b) generated from the Xα calculation of the etidronate ion. Satellite intensity from the Ca(4s), C(2s), and O(2s) regions has been removed from the experimental spectrum. The experimental valence band XPS spectrum for iron etidronate (e) is compared with the spectrum generated (c) from combining the spectrum in (b) with that in Figure 9c (the FeO_2 octahedral unit), and the spectrum generated (d) from combining the spectrum in (b) with that in Figure 9b (the FeO_2 tetrahedral unit).

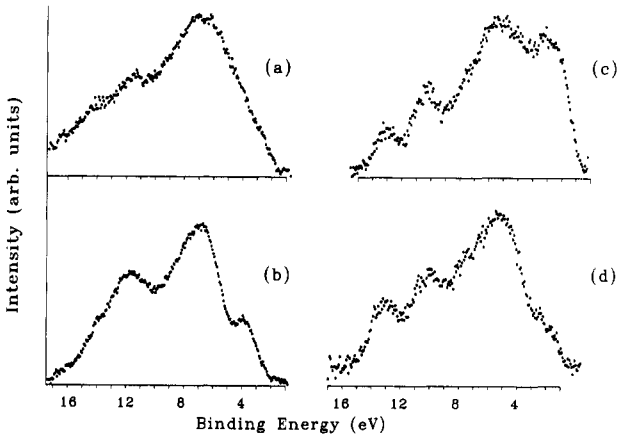

Figure 12. Valence band XPS spectra for the 2-week exposed calcium etidronate treated mild steel plate (a), and after 7 min of etching (c), compared with the spectrum (b) of iron etidronate and (d) ferrous phosphate.

conclusion reached in our previous work.[1] This should now be discussed in more detail. Figure 11 shows a collection of relevant etidronate spectra. First we can see, as discussed previously,[1] that the etidronate ion spectrum can be well understood by a spectrum generated from an Xα calculation of the etidronate ion (Figure 11a,b). The spectrum of iron(III) etidronate (Figure 11e) can also be explained by generating the spectrum by combining the calculated spectrum from etidronate with either an octahedral FeO_2 (Figure 11c) or tetrahedral FeO_2 (Figure 1d) unit. In this case the spectrum corresponding to tetrahedral iron gives significantly better agreement with experiment, so we suggest that iron is in a tetrahedral environment in iron etidronate. When the spectra obtained on exposure of iron or steel to calcium etidronate is compared with that of iron etidronate (Figure 12a,b) considerable similarity is found. However Figure 12a shows a weaker peak at around 12 eV binding energy, together with a broader peak around 5–7 eV binding energy. We believe this is because the film is not simply iron etidronate but a film containing a mixture of oxidized iron and iron etidronate. Comparison of this spectrum with the valence band of FeOOH and Fe_2O_3 (Figure 13) shows that the latter have no sharp features around 12 eV binding energy but have considerable intensity in the low binding energy region 3–6 eV. Thus superimposition of the iron etidronate spectrum with FeOOH and/or Fe_2O_3 would provide a spectrum that agrees with our suggestion.

Oxidation State of the Phosphate. The spectrum of the film after 7 min of etching following medium exposure (2 weeks; Figure 12c) is similar to that of ferrous phosphate, except that there is more intensity at lower binding energy. The greater amount of low binding energy intensity would be expected on the basis of a mixture of oxidized iron as discussed above. Of course it is not possible to actually prove that the phosphate is in the form of iron(II) phosphate rather than iron(III) phosphate, since it would be possible to explain the results by mixing either phosphate in appropriate proportions with the iron oxide spectra. Nevertheless the spectra below 6 eV are very similar, and the results are clearly not inconsistent with

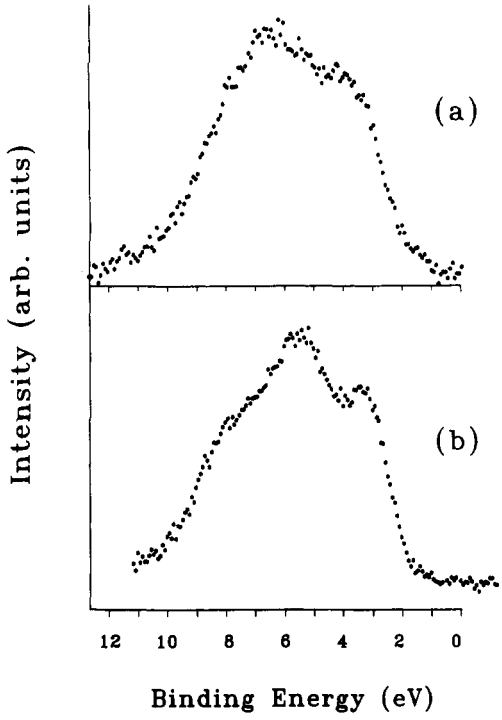

Figure 13. Valence band XPS spectra for (a) FeOOH and (b) Fe_2O_3 from ref 13.

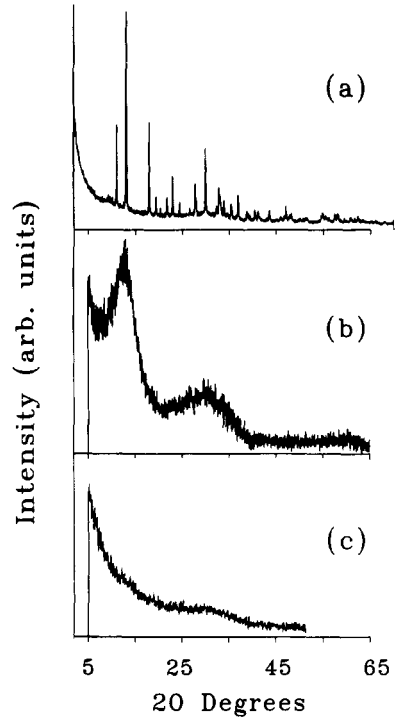

Figure 14. X-ray diffraction patterns for (a) ferrous phosphate ($Fe_3(PO_4)_2 \cdot 8H_2O$), (b) ferrous phosphate after being heated in a vacuum oven for 20 h at 80 °C, and (c) ferrous phosphate after 37 h of analysis in the XPS instrument.

the formation of iron(II) phosphate. We will discuss the significance of iron(II) phosphate in our discussion of the mechanism of the interaction between the inhibitor and the oxide film below.

Composition Differences with Exposure Time. It is interesting to examine the results for different exposure times in more detail in the light of the above discussion. It is clear that the phosphate can be removed after further etching. In the case of the short exposure time (2 h) the spectrum changes to resemble that[31] of FeO and metallic iron after 6 min of etching. In the case of medium exposure time (2 weeks) the thicker film means that even after 127 min of etching the substrate iron is not reached. The phosphate is however removed after some 100 min of etching. The phosphate layer certainly extends to a considerable depth into the film, perhaps because the etidronate steadily interacts with the oxide layer as it grows with time. There will also be some decomposition of the phosphate layer by argon ions, since we did see some decomposition of phosphate samples under argon ion etching. After 127 min of etching the spectrum looks similar to that of Fe_2O_3. In the case of the long exposure time (124 days) no phosphate is seen perhaps because the outer etidronate-rich region increases in thickness and/or the phosphate containing layer falls off the metal surface. It is also notable that the initial spectrum before etching (Figure 4) shows fewer etidronate features, presumably because the spectrum is dominated by iron oxides. Etching causes little change after 12 min, though it is interesting to note that the surface-sensitive spectrum (12(SS) in Figure 4) obtaining by turning the sample to a grazing angle shows a change in the spectrum to appear closer to that of Fe_2O_3, perhaps suggesting that the etching is converting the surface film into Fe_2O_3. We have discussed the dehydration of FeOOH in an earlier publication.[13]

Changes Caused by Exposure to the Spectrometer. It is important to consider what changes have occurred in the materials studied by their being exposed to the high vacuum of the spectrometer and the X-rays. The case of the iron phosphates provide a good example to study because, in the case of iron(III) phosphate, dehydration to give an anhydrous compound causes a change in environment about the iron from octahedral to tetrahedral. Our calculations predict a difference in spectrum for iron in these two different sites. Thus have we changed what we have been examining by spectroscopic study (the main concern of any surface science experiment)? We have used X-ray diffraction to evaluate this situation, for while X-ray diffraction is not normally a particularly surface-sensitive method, we would anticipate the effect of the high vacuum and the X-rays to penetrate substantially into the bulk, even though XPS only examines the surface region. To separate the effect of the high vacuum and the heat from the X-ray gun from that of any possible decomposition caused by the X-rays (most probably the Bremstraalung X-rays, though much of this intensity is removed by the X-ray window), we have studied samples heated in a vacuum oven and compared these with samples after exposure in the XPS instrument. Figure 14 shows the X-ray diffractograms for iron(II) phosphate. In this case the effect of either the vacuum oven or the XPS instrument is to render the initially crystalline material amorphous. Figure 15 shows the X-ray diffractograms for iron(III) phosphate. In contrast we see that either the vacuum oven or the XPS instrument converts the sample into a different, but still crystalline XRD diffractogram. We have compared the diffractograms with that of fully anhydrous iron(III) phosphate obtained by heating metastrengite to 600 °C in an oven but find that the diffractograms are different. Thus it seems reasonable to conclude that while some dehydration occurs, the fully anhydrous form is not formed, and thus it is still reasonable to interpret the spectrum as corresponding to iron in the octahedral form, as has been done above (Figure 10).

We also examined the effect of XPS studies and vacuum oven studies on calcium etidronate. The results implied differences between the effect of changes caused by XPS examination and in the vacuum oven, but the diffracto-

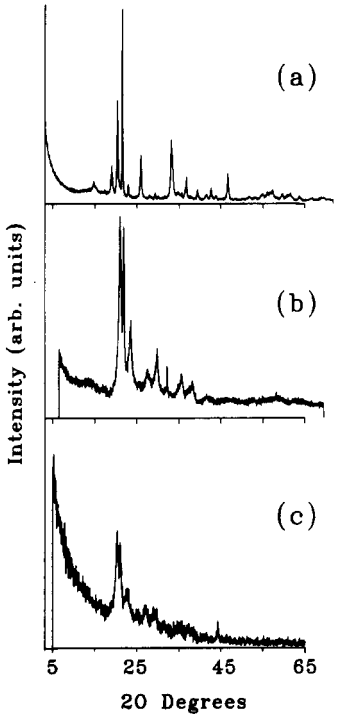

Figure 15. X-ray diffraction patterns for (a) ferric phosphate ($FePO_4 \cdot 2H_2O$), (b) ferric phosphate after being heated in a vacuum oven for 20 h at 80 °C, and (c) ferric phosphate after 28 h of analysis in the XPS instrument.

grams were complex and no clear trends could be identified.

Oxidation of Etidronate by Interaction with the Native Oxide Layer. It is interesting to consider why the etidronate appears to have interacted with the native oxide layer. If we are correct in our suggestion that the phosphate formed is in the form of iron(II) phosphate, then it is possible to conceive of a redox process where the etidronate ion is oxidized to phosphate, and the ferric ions in the outer part of the film are reduced to ferrous ions. We already know that the native formed oxide film on iron and mild steel consists of iron(III) oxides.[29] Thus we might envisage the oxidation of the etidronate occurring by a reaction such as

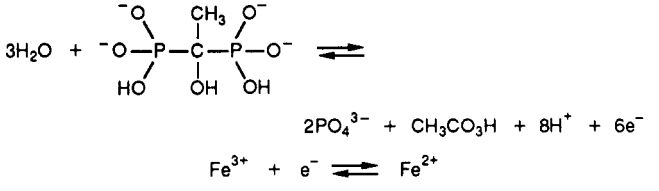

HEDP is normally quite stable, and complexes with metal ions, including Fe^{3+}, can be made without apparent decomposition. However our system involves a solid-state process involving a mixed iron etidronate and iron oxide layer, and these different conditions may be favorable for the above process. It is interesting to note that phosphates have a high affinity for oxidized iron, and this is a key to their role in soils.[30]

Conclusions

The valence band region can be seen, both from the experimental data presented and from the calculations, to be a sensitive probe of subtle chemical changes occurring on the surface of corrosion inhibitor treated iron and mild steel surfaces, a situation where core XPS is of very little value. In particular one sees that the etidronate ion interacts with the native oxide film of the metal. This observation is very interesting, especially as it suggests that one might be able to exploit this type of interaction to improve inhibitor activity. Thus one might be able to extend this approach to the development of an inhibitor which interacts with and removes unprotective oxide films and replaces them with an impervious and protective film. In the case of etidronate the extent of corrosion protection is limited, though the corrosion products are generally colorless, a desirable cosmetic feature in many applications. The work suggests that the interaction might be via an oxidation of the etidronate to phosphate with a corresponding reduction of the iron oxide film.

The ability to distinguish between phosphate and etidronate and the suggestion that one should be able to distinguish between octahedral and tetrahedral iron sites are further evidence of the sensitivity of valence band photoemission. X-ray diffraction studies indicate that the spectral collection process may amorphatize the film as well as dehydrating the film. Such investigations need to be coupled with XPS studies of this type to ensure that the observed changes are not spectrometer induced.

Acknowledgment. This material is based upon work supported by the National Science Foundation under Grant No. CHE-8922538. We are grateful to the U.S. Department of Defense for funding the X-ray diffraction equipment.

Registry No. CaHEDP, 75323-71-6; FeHEDP, 91364-54-4; Fe, 7439-89-6; $Fe_3(PO_4)_2$, 14940-41-1; $FePO_4$, 10045-86-0; steel, 12597-69-2.

(29) Schuetzle, D.; Carter, R. O., III; Shyu, J.; Dickie, A.; Holubka, J.; McIntyre, N. S. *Appl. Spectrosc.* **1986**, *40*, 641.

(30) Stucki, J. W.; Goodman, B. A.; Schwertmann, U. *Iron in Soils and Clay Minerals*; NATO ASI Series C: Mathematical and Physical Sciences, Vol 217, D. Reidel: Dordrecht, Holland, 1988.

(31) McIntyre, N. S.; Zetaruk, D. G. *Anal. Chem.* **1977**, *49*, 1521.